

Preprint: 1–6 (1998)

FOSSIL IMPRINTS OF THE FIRST GENERATION SUPERNOVA EJECTA IN EXTREMELY METAL-DEFICIENT STARS

Toshikazu Shigeyama

Department of Astronomy, School of Science, University of Tokyo, Bunkyo-ku, Tokyo, 113-0033 Japan
Research Center for the Early Universe, School of Science, University of Tokyo, Bunkyo-ku, Tokyo, 113-0033 Japan;
shigeyama@astron.s.u-tokyo.ac.jp

Takuji Tsujimoto

National Astronomical Observatory, Mitaka, Tokyo, 181-8588 Japan;
tsuji@misty.mtk.nao.ac.jp

(Received 8 July 1998; accepted 14 September 1998)

Abstract

Using results of nucleosynthesis calculations for theoretical core-collapse supernova models with various progenitor's masses, it is shown that abundance patterns of C, Mg, Si, Ca, and H seen in extremely metal-deficient stars with $[\text{Fe}/\text{H}] \lesssim -2.5$ follow those seen in the individual first generation supernova remnants (SNRs). This suggests that most of the stars with $[\text{Fe}/\text{H}] \lesssim -2.5$ were made from individual supernova (SN) events. To obtain the ratio of heavy elements to hydrogen, a formula is derived to estimate the mass of hydrogen swept up by a SNR when it occurs in the interstellar matter with the primordial abundances. We use $[\text{Mg}/\text{H}]$ to indicate the metallicities instead of $[\text{Fe}/\text{H}]$. The metallicities $[\text{Mg}/\text{H}]$ predicted from these SNRs range from ~ -4 to ~ -1.5 and the mass of Mg in a SN is well correlated with its progenitor's mass. Thus the observed $[\text{Mg}/\text{H}]$ in an extremely metal deficient star has a correspondence to the progenitor's mass. A larger $[\text{Mg}/\text{H}]$ corresponds to a larger progenitor's mass. Therefore, so called 'age-metallicity relation' does not hold for stars with $[\text{Fe}/\text{H}] \lesssim -2.5$. In contrast, the $[\text{Mg}/\text{Fe}]$ ratios in the theoretical SNRs have a different trend from those in extremely metal-deficient stars. It is also shown that the observed trend of $[\text{Mg}/\text{Fe}]$ can predict the Fe yield of each SN given the correspondence of $[\text{Mg}/\text{H}]$ to the progenitor's mass. The Fe yields thus obtained are consistent with those derived from SN light curve analyses. This indicates that there is still a problem in modelling a core-collapse supernova at its beginning of explosion or mass cut. The abundance determination of O in extremely metal-deficient stars, that have not been done from observational analyses, are strongly desired to test the hypothesis that the elements in an extremely metal-deficient star come from a single SN event and to obtain reliable yields for SNe.

Key words: nucleosynthesis–stars:abundances–stars:Population II–supernovae:general–supernova remnants

the lowest metallicity ($[\text{Fe}/\text{H}] \sim -4$).

1. INTRODUCTION

Recent observations and the analyses imply that the abundance pattern of an extremely metal-deficient star with $[\text{Fe}/\text{H}] (\equiv \log (\text{Fe}/\text{H}) - \log (\text{Fe}/\text{H})_{\odot}) \lesssim -2.5$ may retain information of a preceding single supernova (SN) event or at most a few SNe (McWilliam et al. 1995; Ryan, Norris, & Beers 1996). A theoretical attempt from this point of view has been already made (Audouze & Silk 1995) to explain the observed abundance patterns. They argued that a combination of yields from two SNe with different progenitor's masses at the main sequence (M_{ms}) is consistent with the abundance patterns of stars with

Assuming that the formation of extremely metal-deficient stars is triggered by a single supernova remnant (SNR) and that the formed stars retain the abundance pattern of this SN, one could predict abundance patterns (including hydrogen) of these stars from theoretical SN models available at present (e.g., Woosley & Weaver 1995; Tsujimoto et al. 1995; Nomoto et al. 1997). In this *letter*, we will compare the abundance pattern thus obtained with observations to test whether the chemical enrichment by individual SNRs could explain the observed abundances on the surfaces of extremely metal-deficient stars. We will use models in Woosley & Weaver (1995) (referred to WW95) and those in Tsujimoto et al. (1995)

and Nomoto et al. (1997) (T95).

The metallicity of a star has been usually indicated by $[\text{Fe}/\text{H}]$. On the other hand, the yields of Fe from SN models to date have not converged (Woosley & Weaver 1995; Tsujimoto et al. 1995) because of uncertainties in the explosion mechanism and fall back dynamics or mass cut between the forming neutron star (or black hole) and the ejected envelope (e.g., Thielemann, Hashimoto, & Nomoto 1990). Thus the yields of lighter α -elements are more reliably calculated. We will use $[\text{Mg}/\text{H}]$ instead of $[\text{Fe}/\text{H}]$ to specify the metallicity because of the following reasons:

1. Mg is less affected by the mass cut in SN models than Fe.
2. Mg is not synthesized or broken by the SN shock.
3. The mass of ejected Mg increases with increasing progenitor's mass.
4. The abundance of Mg is observationally derived for many stars with $[\text{Fe}/\text{H}] \lesssim -2.5$.

There is a disadvantage in this element, that is, two SN models (WW95 and T95) give somewhat different masses of Mg as a function of progenitor's mass (squares in Fig. 1). The best element to be used in this respect would be O (pentagons in Fig. 1) if O abundances were available for many stars with $[\text{Fe}/\text{H}] \lesssim -2.5$ (see McWilliam et al. 1995; Ryan et al. 1996).

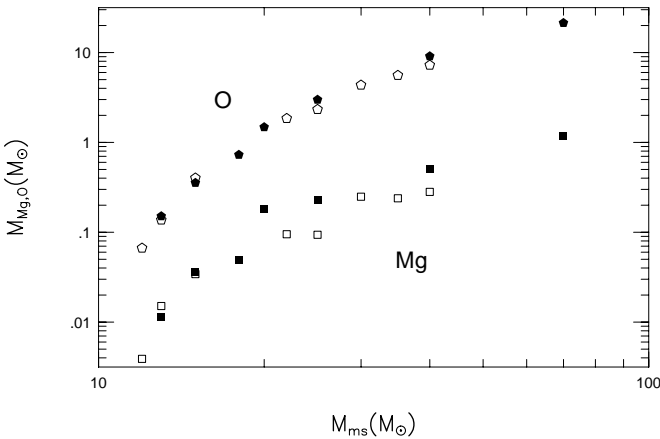


Fig. 1. The masses of Mg (circles) and O (pentagons) ejected from SN models are plotted as a function of the progenitor's mass (Woosley & Weaver 1995 (open); Tsujimoto et al. 1995 (filled)).

There is a clear trend in the observed $[\text{C}/\text{Mg}]$ – $[\text{Mg}/\text{H}]$ plot (crosses in Fig. 2) for $[\text{Mg}/\text{H}] < -2$ that cannot be reconciled with the conventional one-zone models of the Galactic chemical evolution that assume a complete

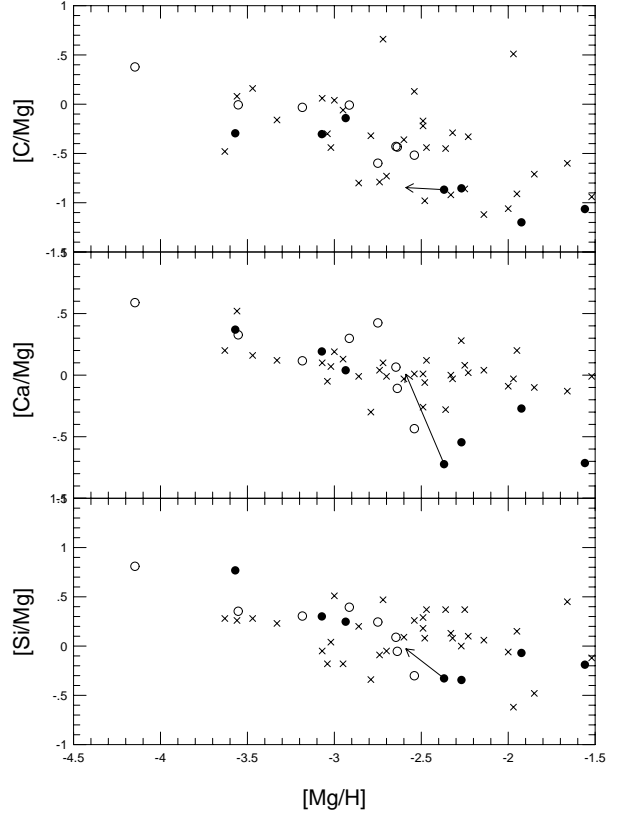


Fig. 2. The top panel: the crosses are the observed $[\text{C}/\text{Mg}]$ for stars plotted against the $[\text{Mg}/\text{H}]$ (McWilliam et al. 1995). The open and filled circles show the same quantities in the first generation SNRs calculated from theoretical SN models (Woosley & Weaver 1995 (open circles); Tsujimoto et al. 1995 (filled circles)). The arrow indicates the change in the abundance pattern of the model to reproduce the SN 1987A observations (Thielemann et al. 1990 and references therein). The middle panel: Same as the top panel but for $[\text{Ca}/\text{Mg}]$. The bottom panel: Same as the top panel but for $[\text{Si}/\text{Mg}]$. See the text for arrows.

mixing of elements inside the Galaxy.¹ The difference of the observed $[\text{C}/\text{Mg}]$ in the range of $-3.5 \lesssim [\text{Mg}/\text{H}] \lesssim -2$ gives a mean gradient $\Delta[\text{C}/\text{Mg}]/\Delta[\text{Mg}/\text{H}] \sim -0.7$. On the other hand, the one-zone Galactic chemical evolution model using T95 would predict the evolutionary change in $[\text{C}/\text{Mg}]$ starting with the value of ~ -1.2 given by the most massive star $M_{\text{ms}} \sim 50 M_{\odot}$ and converging to the average value of ~ -0.9 integrated for stars in the mass range of $10 < M_{\text{ms}}/M_{\odot} < 50$ over the Salpeter initial mass function (IMF) with a slope of $x = -1.35$. It results in the corresponding gradient of $\Delta[\text{C}/\text{Mg}]/\Delta[\text{Mg}/\text{H}] \sim +0.2$ that has the opposite sign and a smaller absolute

¹However, Audouze & Silk (1995) have deduced that the chemical inhomogeneity is maximal in the range $-4 \lesssim [\text{Fe}/\text{H}] \lesssim -2.5$ ($-3.5 \lesssim [\text{Mg}/\text{H}] \lesssim -2$).

value than in observations. This argument also holds for WW95. If we introduce a metallicity-dependent IMF, the observed gradient requires a drastic change of the slope of the IMF from $x \sim -10$ at $[\text{Fe}/\text{H}] \sim -4$ to $x \sim +0.5$ at $[\text{Fe}/\text{H}] \sim -2.5$. The index of $x \sim -10$ is almost equivalent to assuming that most of the stars with $[\text{Fe}/\text{H}] \sim -4$ are formed from SNRs with $M_{\text{ms}} = 10 M_{\odot}$. It will be shown in the following section that this is indeed the case if we assume that most of the stars with $[\text{Fe}/\text{H}] \lesssim -2.5$ are formed from individual SN events.

Here we will also predict the Fe yields as a function of M_{ms} using the observed $[\text{Mg}/\text{Fe}]$ – $[\text{Mg}/\text{H}]$ trend combined with the $[\text{Mg}/\text{H}]$ – M_{ms} relation in theoretical SN models. Then these Fe yields are compared with those derived from SN light curve analyses. To calculate the mass of hydrogen swept up by a SNR, that is important to obtain $[\text{Mg}/\text{H}]$, the analytical expression for this mass in Cioffi, McKee, & Bertschinger (1988) is modified to be applicable to SNRs that occur in a metal-free interstellar matter (ISM).

2. LATE STAGE EVOLUTION OF THE FIRST GENERATION SUPERNOVA REMNANTS

In a spherically symmetric SNR (e.g., Cioffi et al. 1988), after the radiative cooling time scale becomes shorter than the dynamical time scale at the shock front, the shock front propagates considerably slower than before and makes a dense shell immediately behind it. Most of the mass inside the shock front resides in this shell. The ejecta that contain heavy elements occupy only a small central portion of the SNR even during this pressure driven snowplow (PDS) phase. In a realistic SNR, the situation is different. First, the contact surface between the ejecta and the ISM is subject to the Rayleigh-Taylor instability during the preceding Sedov-Taylor phase (Taylor 1950; Sedov 1959). A large part of the ejecta penetrates into the ISM. Thus it is expected that the ejecta already approach the dense shell at the beginning of the PDS phase and merge with it during this phase. Secondly, an isothermal shock front is considered to be dynamically unstable (Vishniac 1983). Thus the dense shell behind the shock front is fragmented into a number of cloud cores that retain the abundance pattern of the SN. These cloud cores embedded in a high ambient pressure become seeds of stars of the next generation (Nakano 1998). Some of the stars thus formed are currently observed as extremely metal-deficient stars. Accordingly, the average abundance pattern inside the SNR is assumed to represent that in all these stars.

Cioffi et al. (1988) obtained the time t_{merge} when a SNR loses its identity. This time is a function of the ratio of the shock velocity to the sound speed C_s (or the

velocity dispersion) of the ISM at the beginning of PDS phase ($t = t_{\text{PDS}}$) and t_{PDS} itself. For a SNR in a homogeneous ISM with the density of n_1 , t_{PDS} is determined by equation

$$\frac{1}{n_1} \frac{\partial e}{\partial t} = -\alpha \times \Lambda(T), \quad (1)$$

where e and $\Lambda(T)$ are the internal energy and the cooling function at the temperature T , respectively. All the variables are evaluated at the shock front using Sedov-Taylor solutions for the point explosion with the energy E_0 and the number density n_1 . The constant α should be equal to 1.85 to reproduce t_{PDS} for the numerical simulation in Cioffi et al. (1988) when $\Lambda(T)$ for the solar abundances is used. Then $\Lambda_{\text{primordial}}(T)$ is constructed for the gas composed of only hydrogen and helium with their mass ratio $X_{\text{H}} : X_{\text{He}} = 0.75 : 0.25$ under the collisional ionization equilibrium. For $n_1 \gtrsim 10^{-2} \text{ cm}^{-3}$, equation (1) gives T greater than 10^5 K . Thus the ionization of hydrogen does not affect the dynamics.

The mass of hydrogen M_{sw} thus obtained with $\Lambda(T) = \Lambda_{\text{primordial}}(T)$ in equation (1) is approximated by the formula

$$M_{\text{sw}} = 5.1 \times 10^4 M_{\odot} \left(\frac{E_0}{10^{51} \text{ erg}} \right)^{0.97} n_1^{-0.062} \left(\frac{C_s}{10 \text{ km s}^{-1}} \right)^{-9/7}. \quad (2)$$

The mass M_{sw} is insensitive to n_1 . The sound speed C_s was assumed to be 10 km s^{-1} (or $T \sim 10^4 \text{ K}$). This mass depends on E_0 and n_1 in a different way from that of Cioffi et al. (1988) due to the different cooling function used here. The cooling function with the primordial abundances is approximately proportional to T^{-2} instead of $T^{-1/2}$ in Cioffi et al. (1988).

3. ABUNDANCE PATTERNS

Here we assume that all the stars with $[\text{Mg}/\text{H}] < -2$ are made from individual SNRs. Abundance patterns in individual SNRs will be calculated based on yields from theoretical SN models and compared with those on the surface of metal-deficient stars obtained by McWilliam et al. (1995). For SN models in metal-free environment, we use models Z12A, Z13A, Z15A, Z22A, Z30B, Z35C, Z40C in WW95 to retain the monotonicity of the mass of Mg as a function of progenitor's mass (see filled squares in Fig. 1). Another group of SN models are taken from T95 in which the initial metallicity is solar. Parameters of both models are listed in Table 1.

We divide elements into two categories. One category is composed of the elements not (or at least less) affected by the mass cut in SN models. The examples are C, Mg, Si, and Ca. The other is composed of those affected

Table 1. Input parameters in SN models and the calculated [Mg/H] ratios in the corresponding SNRs (see text for details).

WW95				T95		
Name	$M_{\text{ms}} (M_{\odot})$	$E_0 (10^{51} \text{ erg})$	[Mg/H]	$M_{\text{ms}} (M_{\odot})$	$E_0 (10^{51} \text{ erg})$	[Mg/H]
Z12A	12	1.28	-4.1	13	1	-3.6
Z13A	13	1.29	-3.6	15	1	-3.1
Z15A	15	1.27	-3.2	18	1	-2.9
Z22A	22	1.26	-2.8	20	1	-2.4
Z25B	25	1.83	-2.9	25	1	-2.3
Z30B	30	2.06	-2.5	40	1	-1.9
Z35C	35	2.49	-2.6	70	1	-1.6
Z40C	40	3.01	-2.6	-	-	-

by the mass cut and includes Cr, Mn, Fe, Co, Ni, for example. This division is necessary because the mass cut in SN models to date is totally artificial and uncertain.

Elements not influenced by mass cut— The yields of elements not influenced by the mass cut are expected to be more reliably calculated in SN models than those influenced by the mass cut. Therefore observed abundance ratios of [C/Mg], [Ca/Mg], [Si/Mg] with respect to [Mg/H] (Fig. 2) can tell whether extremely metal-deficient stars were formed from individual SNe. These abundance ratios derived from SN models (open circles: WW95; filled circles: T95) are also plotted in the same figure, in which [Mg/H] is calculated from the ratio of the mass of Mg in a SNR to that of hydrogen swept up by the same SNR (see equation (2)). The relations between [Mg/H] and M_{ms} are shown in Table 1 for both SN models. The values of [Mg/H] for $M_{\text{ms}} \sim 10 M_{\odot}$ (the lower mass limit of the core-collapse SN progenitor) from both models are not so far from the observed lowest value of [Mg/H] ~ -3.7 and the metallicity [Mg/H] increases with increasing progenitor mass M_{ms} . This infers that there are more stars at lower metallicities according to an IMF that decreases toward high masses if stars with lower masses, say $10 M_{\odot}$, explode in the regions that have not been polluted by other SNRs before. This condition is represented as $n_{\star} V_{\text{SNR}} \int_{10 M_{\odot}}^{50 M_{\odot}} \phi(m) dm < 1$ star. Here n_{\star} , ϕ , and V_{SNR} denote the number density of the first generation stars, the IMF normalized to unity between the lower and upper mass limits, and the maximum volume occupied by a single SNR, respectively. This condition results in a star formation efficiency for the first generation stars smaller than 2%, if the Salpeter IMF is used.

A trend seen in the observed [C/Mg] (crosses in the top panel of Fig. 2) is well reproduced by both models. This means that stars with [Mg/H] ~ -3.5 were made from individual low mass ($M_{\text{ms}} \sim 10 M_{\odot}$) SNe and that stars with [Mg/H] ~ -2 were from individual high mass SNe ($M_{\text{ms}} \sim 50 M_{\odot}$). For [Si/Mg], both models are also consistent with observations, though the observed [Si/Mg]

has no clear trend. The [Ca/Mg] ratios derived from T95 with $M_{\text{ms}} \geq 20 M_{\odot}$ deviate from observations and gives lower values in the region [Mg/H] > -2.5 . This indicates that the yields of Ca of T95 with $M_{\text{ms}} \geq 20 M_{\odot}$ are too small. These abundance patterns together with the predicted [Mg/H] ratios in Table 1 suggest that stars with $-3.5 \lesssim [\text{Mg}/\text{H}] \lesssim -2$ are made from individual SN events.

Elements influenced by mass cut— The upper panel of Fig. 3 shows that the [Mg/Fe] ratios derived from both models do not follow the observations. This reconfirms that none of the two models correctly describes the dynamics and/or nucleosynthesis near the surface of the Fe core in progenitor stars during explosion. In both models, less massive stars have too large Fe yields. More massive stars in T95 have too small Fe yields but the opposite is the case for WW95. The lower panel of Fig. 3 shows that the [Ca/Fe] ratios from both models are smaller than the observations. This can be ascribed to too large Fe yields from less massive stars of theoretical models again. An apparent fit of the observational data to the model for [Mg/H] > -2.5 is a consequence of two errors in yields of both Ca (see section 3) and Fe for more massive stars (see the next section).

Abundances of some heavy elements in the ejecta of the $20 M_{\odot}$ supernova were deduced from the SN 1987A observations (Thielemann et al. 1990 and references therein). As the mass of Mg ejected from SN 1987A was not estimated from observations, we derive the mass of Mg by reducing the value of T95 to match the observed [Mg/Fe] ratio in extremely metal-deficient stars. The corresponding change of [Mg/Fe] is shown by the arrow in the upper panel of Fig. 3. If we use the mass of Mg thus derived and the observed masses of C, Si, Fe, and Ca (the upper limit), the abundance ratios of the model with $M_{\text{ms}} = 20 M_{\odot}$ would move following the arrows in Fig. 2 and in the lower panel of Fig. 3. Thus the abundance pattern of the best observed SN coincides with that in extremely metal-deficient stars with [Mg/H] ~ -2.6 and the mass of Mg in the $20 M_{\odot}$ model of T95 might be

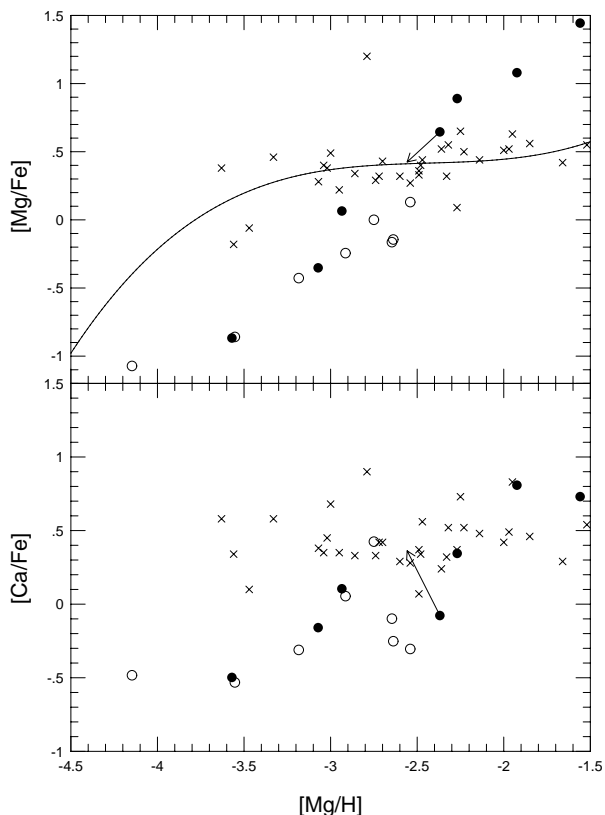


Fig. 3. The upper panel: the crosses are the observed $[\text{Mg}/\text{Fe}]$ for stars plotted against the $[\text{Mg}/\text{H}]$ (McWilliam et al. 1995). The solid curve shows the χ -square fit of the observed points with the errors given in McWilliam et al. (1995) to a cubic polynomial formula. The open and filled circles show the same quantities in the first generation SNRs calculated from theoretical SN models (Woosley & Weaver 1995 (open circles); Tsujimoto et al. 1995 (filled circles)). The lower panel: Same as the top panel but for $[\text{Ca}/\text{Fe}]$. See the text for arrows.

overestimated.

4. IRON YIELDS DEDUCED FROM EXTREMELY METAL DEFICIENT STAR OBSERVATIONS

We will reverse the argument in the preceding sections. Suppose that the trends in the observed abundance ratios, say $[\text{Mg}/\text{Fe}]$, tell yields of SNe as a function of $[\text{Mg}/\text{H}]$. The χ^2 fit of the observational data to a cubic polynomial formula gives the solid curve in the upper panel of Fig. 3. This curve and $[\text{Mg}/\text{H}]$ of each model predict the mass of Fe (M_{Fe}) from a SN as a function of M_{ms} . Filled circles in Fig. 4 show the predicted Fe masses using T95. These Fe masses are completely different from those given in the original models (triangles)

but hardly change the average Fe yield integrated over the Salpeter IMF. Open circles are those from WW95 and give a similar amount of Fe for each progenitor's mass. Points with error bars also shown in the same figure are the Fe masses obtained from SN light curve analyses. Good fits of the Fe masses from the light curve analyses to those inferred from the abundance patterns demonstrate that this procedure to obtain the Fe yields works, if the Fe yields are not affected by the initial metallicities. A discrepancy of Fe masses at $M_{\text{ms}} \sim 10 M_{\odot}$ might be due to the small number of fairly scattered observed points of $[\text{Mg}/\text{Fe}]$ at $[\text{Mg}/\text{H}] \sim -3.5$ in the upper panel of Fig. 3. The Fe yields thus obtained predict that the lowest $[\text{Fe}/\text{H}]$ should be ~ -3.7 for both models.

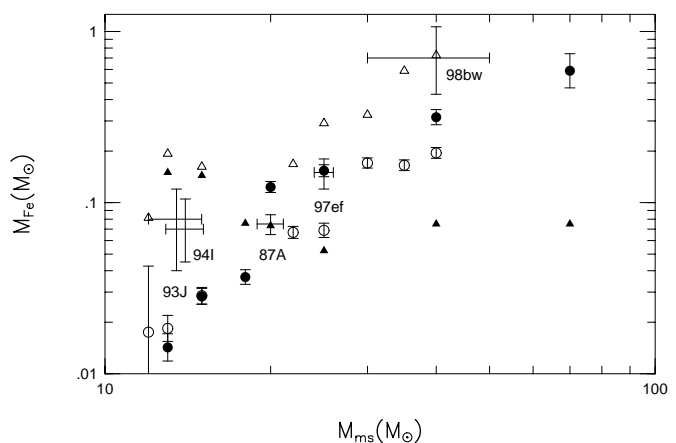


Fig. 4. The masses of Fe in SN models (Woosley & Weaver 1995 (open); Tsujimoto et al. 1995 (filled)) are shown by triangles. Circles show the masses of Fe in SN models with 1σ error bars of the χ^2 fit in the upper panel of Fig. 3. These masses are determined by the $[\text{Mg}/\text{Fe}]$ – $[\text{Mg}/\text{H}]$ relations indicated with the solid curve in the upper panel of Fig. 3 and the $[\text{Mg}/\text{H}]$ – M_{ms} relations. Points with error bars are the masses of ^{56}Ni , that eventually decays to ^{56}Fe derived from SN light curve analyses (SN 1987A: Shigeyama & Nomoto 1990; SN 1993J: Shigeyama et al. 1994; SN 1994I: Iwamoto et al. 1994; SN 1997ef: Iwamoto et al. 1998a; SN 1998bw: Iwamoto et al. 1998b).

5. CONCLUSIONS

We have shown that the abundance patterns of C, Mg, Si, Ca, and H theoretically predicted in the first generation SNRs are in good agreement with those observed in extremely metal-deficient stars with $-4 < [\text{Fe}/\text{H}] < -2.5$. All these elements are thought to be less affected by the mass cut in SN modelling than heavier elements like Fe. This agreement implies that each extremely metal-deficient star was formed from a single SN event. In contrast, both theoretical SN models predict different trends

in the $[\text{Mg}/\text{Fe}]-[\text{Mg}/\text{H}]$ plot from the observed one. Conversely, the mass of Fe ejected by each SN as a function of M_{ms} can be derived from the observed $[\text{Mg}/\text{Fe}]-[\text{Mg}/\text{H}]$ trend combined with the $[\text{Mg}/\text{H}]-M_{\text{ms}}$ relation in theoretical SN models. This M_{Fe} as a function of M_{ms} is consistent with that derived from SN light curve analyses. Following the same procedure presented in this *letter* to obtain the Fe yields, we can derive the yields for other elements such as Ti, Cr, Mn, Co, Ni and r-process elements (Tsujimoto & Shigeyama 1998), all of which are very uncertain in SN models. If O abundances are deduced in extremely metal-deficient stars, we will be able to obtain more reliable yields for SNe. In the forthcoming paper we will also discuss the connection between the chemical enrichment by individual SNe and the subsequent chemical evolution.

We are grateful to the anonymous referee for making useful comments. This work has been partially supported by COE research (07CE2002) of the Ministry of Education, Science, Culture, and Sports in Japan.

References

- Audouze, J. & Silk, J. 1995, *ApJ*, 451, L49
- Cioffi, D. F., McKee, C. F., & Bertschinger, E. 1988, *ApJ*, 334, 252
- Iwamoto, K., Nomoto, K., Höflich, P., Yamaoka, H., Kumagai, S., & Shigeyama, T., 1994, *ApJ*, 437, L115.
- Iwamoto, K., Nakamura, T., Nomoto, K., Mazzali, P. A., Garnavich, P., Kirshner, R., Jha, S., Balam, D. 1998, *ApJ*, submitted
- Iwamoto, K., et al. 1998, *Nature*, in press
- McWilliam, A., Preston, G. W., Sneden, C., & Searle, L. 1995, *AJ*, 109, 2757
- Nakano, T. 1998 *ApJ*, 494, 587
- Nomoto, K., Hashimoto, M., Tsujimoto, T., Thielemann, F.-K., Kishimoto, N., Kubo, Y., & Nakasato, N. 1997, *Nucl. Phys. A*, 616, 79c
- Ryan, S. G., Norris, J. E., & Beers, T. C. 1996, *ApJ*, 471, 254
- Sedov, L. I., 1959, in *Similarity and Dimensional Methods for Initial-Value Problems*, (New York: Wiley-Interscience)
- Shigeyama, T., & Nomoto, K. 1990, *ApJ*, 360, 242
- Shigeyama, T., Suzuki, T., Kumagai, S., Nomoto, K., Saio, H., & Yamaoka, H. 1994, *ApJ*, 420, 341
- Sneden, C., Pilachowski, C. A., VandenBerg, D. A. 1986, *ApJ*, 311, 826
- Taylor, G. I., 1950, *Proc. Roy. Soc. London A*, 201, 159
- Thielemann, F.-K., Hashimoto, M., & Nomoto, K. 1990, *ApJ*, 349, 222
- Tsujimoto, T., Nomoto, K., Yoshii, Y., Hashimoto, M., Yanagida, S., & Thielemann, F.-K. 1995, *MNRAS*, 277, 945
- Tsujimoto, T., & Shigeyama, T. 1998, submitted to *ApJ*
- Turatto, M., et al. 1998, *ApJ*, 498, L129
- Vishniac, E. T. 1983, *ApJ*, 274, 152
- Woosley, S. E., Weaver, T. A. 1995, *ApJs*, 101, 181